A critical approach to the determination of optimal heat rejection pressure in transcritical systems

Luca Cecchinato, Marco Corradi, Silvia Minetto

Accepted Manuscript

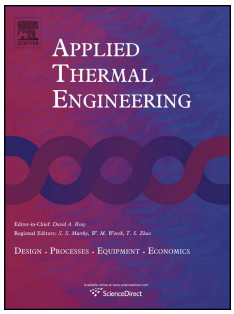

Title: A critical approach to the determination of optimal heat rejection pressure in transcritical systems

Authors: Luca Cecchinato, Marco Corradi, Silvia Minetto

PII: S1359-4311(10)00178-X

DOI: 10.1016/j.applthermaleng.2010.04.015

Reference: ATE 3075

To appear in: *Applied Thermal Engineering*

Received Date: 9 March 2010

Accepted Date: 12 April 2010

Please cite this article as: L. Cecchinato, M. Corradi, S. Minetto. A critical approach to the determination of optimal heat rejection pressure in transcritical systems, Applied Thermal Engineering (2010), doi: 10.1016/j.applthermaleng.2010.04.015

A critical approach to the determination of optimal heat rejection pressure in transcritical systems

Luca Cecchinato[1], Marco Corradi[*,1], Silvia Minetto[2]

Dipartimento di Fisica Tecnica, Università di Padova, via Venezia 1, I-35131 Padova, Italy

Abstract

In this paper the optimal energy efficiency and high cycle pressure problem in single stage refrigerating carbon dioxide vapour compressor units operating in transcritical conditions is addressed. Literature approximated solutions to the optimisation problem are analysed and critically discussed. A numerical model for CO_2 heat exchangers and refrigerant systems is developed. Different gas coolers are simulated in order to investigate the effect of literature simplifying assumptions on the optimal pressure determination: the analysis showed a strong sensitivity of the gas cooler outlet temperature from the secondary fluid temperature, from its capacity rate and from the heat exchanger geometry. Nevertheless it resulted that approximated solutions obtained considering the

[*] **Corresponding author.** Tel.: +39 049 827 6882; fax: +39 049 827 6896; e-mail: marco.corradi@unipd.it

[1] Junior Member of IIR Commission B2

[2] Junior Member of IIR Commission D1

carbon dioxide gas cooler outlet temperature as an independent variable behaved better than solutions correlating it to secondary fluid inlet temperature.

A commercial refrigeration plant and a heat pump water heater were finally simulated to verify their energy performances when applying literature approximated solutions in presence of an on-board compressor capacity and supply water temperature control respectively. While in the case of the commercial refrigeration plant no major penalisation resulted from the literature approximated solutions simplifying assumptions, the heat pump performance was strongly deteriorated, up to -30%, as a consequence of the huge variation in the water capacity flow rate resulting from the water temperature control.

It was finally concluded that an approximated correlation should be critically evaluated before implementation; a real-time algorithm for determining the optimal (or quasi-optimal) pressure value could provide a more efficient and robust solution.

Keywords: CO_2, Transcritical cycle, Optimisation, Refrigeration, Heat pump, Gas cooler.

Nomenclature

$\dot{C}$	heat capacity rate ($W \cdot K^{-1}$)	*Subscripts*	
C	constant	*c*	gas cooler outlet
COP	coefficient of performance	*Chen*	approximated *Chen* and Gu [20] solution
h	enthalpy ($kJ \cdot kg^{-1}$)	*d*	compressor discharge
HDF	heat dissipation factor (-)	*e*	evaporator
IHX	internal heat exchanger (-)	*gc*	gas cooler

K	constant	*hs*	gas cooler secondary fluid
$\dot{m}$	refrigerant mass flow rate ($kg \cdot s^{-1}$)	*hsr*	evaporator secondary fluid
p	pressure (10^5 Pa)	*i*	inlet
Q	cooling load (W)	*ihx*	internal heat exchanger
T	temperature (℃)	*is*	isentropic
$\dot{V}$	swept volume ($m^3 \cdot h^{-1}$)	*Kauf*	approximated *Kauf* [16] solution
x	quality (-)	*Liao*	approximated Liao et al.[17] solution
		o	outlet
Greek symbols		*opt*	optimal
ΔT_{SH}	superheat (K)	*Sarkar*	approximated *Sarkar* [18] et al. solution
ε	heat exchanger efficiency (-)	*v*	volumetric
η	compressor efficiency (-)		
ρ	density ($kg \cdot m^{-3}$)		
Φ	geometric characteristic (-)		

1. Introduction

Carbon dioxide is one of the oldest refrigerants, as it was already employed at the end of the nineteenth century, mainly where safety was essential. After a long decline, due to the came into use of synthetic refrigerants, at the end of the past century CO_2 was revived thanks to its very low environmental impact. In 1994, the Norwegian professor Gustav Lorentzen [1] first proposed again this refrigerant as a working fluid for vapour compression inverse cycles and from that moment many other Authors have extensively studied such applications. The contributions of Cavallini and Nekså [2], Nekså [3], Groll [4], Cecchinato et al. [5] and Kim et al. [6] appear to deserve a mention within the scope of the present paper.

CO_2 is seen as an effective solution to the problem of the ozone depletion and

of the direct contribution to the global warming of anthropic origin, since its ODP is zero and its GWP is negligible. However, the CO_2 transcritical simple vapour compression inverse cycle poor energy efficiency, when compared with a traditional subcritical cycle, especially for some applications, might result in a higher indirect contribution to the global warming of anthropic origin.

Experimental results in the automotive sector ([7], [8]) and in commercial refrigeration applications ([9], [10]) show that it is possible to compete with state-of-the-art HFC systems energy efficiency. Carbon dioxide operating according to a transcritical cycle is regarded as an energy efficient option also for heat pump water heaters: the gas cooling process well fits the temperature profile of a finite water stream during heating, resulting in a quite large temperature lift in water without significant penalisation in the cycle coefficient of performance (COP), as it was clearly demonstrated in the technical literature ([3], [11], [12], [13]).

In general terms an inverse CO_2 operated cycle is very different from a traditional one since the high pressure is often supercritical and the resulting refrigerating cycle does not entail condensation, but a simple cooling process of dense fluid accomplished in the so-called ‘gas cooler’. As a consequence, unlike the common subcritical cycle, the flow factor of the expansion valve determines the gas cooler pressure, which is no more related only to the temperature of the heat transfer process. Then for the best utilisation of such a technology it is necessary that in each working condition the system operates at optimal value of the cycle high pressure, that is the one which leads to the maximum COP ([1], [6], [14]).

Several Authors, Inokuty [15], Kauf [16] , Liao et al. [17], Sarkar et al. [18], Sarkar et al. [19] and Chen and Gu [20] faced up the optimisation problem of a

transcritical system high pressure. By means of different simplifying assumption, the same Authors theoretically worked out expressions to define the optimal cycle high pressure as a function of the refrigerating cycle variables, which are mainly the gas cooler refrigerant outlet temperature and the evaporating temperature. Cabello et al. [21] compared optimal gas cooler pressures of an experimental plant with the proposed relations, finding significant deviations between the experimental and calculated values.

In this paper the approximated optimisation problem solutions are analysed and the simplifying hypotheses are critically discussed. In Section 2, the problem of optimal rejection pressure determination is discussed. In Section 3 a numerical model for CO_2 heat exchangers and refrigerant systems is introduced. In Section 4 different gas coolers are simulated varying the heat exchanger heat transfer area and the heat rejection fluid temperature and heat capacity rate. The optimal pressure values are numerically obtained and compared to the theoretical expressions proposed by the formerly cited Authors. In Section 5 both a commercial refrigeration plant and a heat pump water heater are simulated in order to find optimal pressure values under variable working conditions and to compare these values with the approximated solutions. Conclusions are drawn in Section 6.

2. The optimal heat rejection pressure

2.1 Problem definition

The reference transcritical carbon dioxide circuit is presented in Figure 1. The p-

h diagram of the corresponding inverse cycle is represented in Figure 2 pointing out a non-isentropic and non-adiabatic compression process (1-2d), a non-isobaric heat rejection process in the gas cooler (2d-3) and an isobaric heat rejection process (3-3') in the internal heat exchanger (IHX) high pressure side, both of them taking place in the high pressure side. An adiabatic expansion process (3'-4'), an isobaric evaporation process (4'-1') and an isobaric heating process (1'-1) occurring in IHX low pressure side are further shown. The theoretical coefficient of performance (*COP*) of this cycle is defined as:

$$COP = \frac{h_{1'} - h_{3'}}{h_2 - h_1} = \frac{h_1 - h_3}{h_2 - h_1} = \eta_{is} \frac{h_1 - h_3}{h_{2s} - h_1}, \quad (1)$$

where (1-2s) represents adiabatic reversible compression process, (1-2) corresponds to a irreversible adiabatic compression process and the isentropic efficiency of the compressor, η_{is}, is defined as following:

$$\eta_{is} = \frac{h_{2s} - h_1}{h_2 - h_1}, \quad (2)$$

Considering the transcritical refrigerating unit represented in Figure 1, the following simplifying hypothesis have been assumed:

1) isentropic and volumetric compression efficiency are influenced only by the compression pressure ratio and, for the range of variation of this parameter, a linear variation can be considered;
2) constant gas cooler heat sink fluid mass flow rate and specific heat at constant pressure;
3) constant evaporator secondary fluid mass flow rate and specific heat at constant pressure;
4) negligible refrigerant pressure drops in refrigerant lines (compressor discharge and suction lines, liquid line after the gas cooler).

The system represented in Figure 1 is ideally equipped with an accumulator that can manage the refrigerant charge variation occurring in each component, so that there is no influence of the refrigerant charge on the cycle pressures, and so on the optimal high pressure. The accumulator has not been represented, as it can be located in different places of the circuit, as it will be detailed in section 5.

The evaporator outlet point (1' in Figure 2) has been represented in the superheated vapour region, depending on the chosen application it could be also in the two-phase or saturated zone. In this case, please consider the evaporator outlet quality variable, $x_{e,o}$, instead of the evaporator outlet superheat value, $\Delta T_{SH,e}$, which is used in the following.

Now, expressing the enthalpies in terms of the corresponding pressures and temperatures the following relations can be written:

$$h_1 = h_1(p_e, T_1), \tag{3}$$

$$h_{2s} = h_{2s}(p_d, p_e, T_1), \tag{4}$$

$$h_3 = h_3(p_c, T_3). \tag{5}$$

where p_d, p_c and p_e are the pressure values at the compressor discharge, gas cooler outlet and evaporator outlet respectively. The heat dissipation factor, *HDF*, can be now introduced to account for the heat rejection process of the compressor crankcase to the surrounding environment, or to a cooling fluid, as a function of the specific compression work:

$$HDF = \frac{h_2 - h_{2d}}{h_2 - h_1} = \eta_{is} \frac{\left(h_1 + \frac{h_{2s} - h_1}{\eta_{is}}\right) - h_{2d}}{h_{2s} - h_1} = 1 - \frac{h_{2d} - h_1}{h_{2s} - h_1}, \tag{6}$$

the following equation can be deduced for the gas cooler inlet refrigerant enthalpy:

$$h_{2d} = h_1 + \frac{1-HDF}{\eta_{is}}\left[h_{2s}(p_d, p_e, T_1) - h_1\right]. \quad (7)$$

The compressor discharge pressure and gas cooler outlet pressure are related by the following implicit equation accounting for gas cooler pressure drops:

$$p_d - p_c = f\left(p_d, h_{2d}, \dot{m}, T_{hs,i}, \dot{C}_{hs}, \Phi_{gc}\right), \quad (8)$$

The heat capacity rate $\dot{C}_{hs}$ is mass flow rate multiplied by specific heat. Considering p_c as an independent variable equation (8) can be written as:

$$p_d = p_d\left(p_c, h_{2d}, \dot{m}, T_{hs,i}, \dot{C}_{hs}, \Phi_{gc}\right), \quad (9)$$

Considering (4), (7) and (9), the following functions for the suction temperature, T_1, for the high pressure side IHX outlet enthalpy, $h_{3'}$, for the suction pressure and for the gas cooler outlet temperature, p_e and T_3, are introduced:

$$T_1 = T_1\left(p_c, p_e, T_3, \Delta T_{SH,e}, \dot{m}, \Phi_{ihx}\right), \quad (10)$$

$$h_{3'} = h_{3'}\left(p_c, p_e, T_3, \Delta T_{SH,e}, \dot{m}, \Phi_{ihx}\right), \quad (11)$$

$$p_e = p_e\left(h_{3'}, \Delta T_{SH,e}, \dot{m}, T_{hsr,i}, \dot{C}_{hsr}, \Phi_e\right) = p_e\left(p_c, T_3, \Delta T_{SH,e}, \dot{m}, T_{hsr,i}, \dot{C}_{hsr}, \Phi_e, \Phi_{ihx}\right), \quad (12)$$

$$T_3 = T_3\left(p_c, p_d, h_{2d}, \dot{m}, T_{hs,i}, \dot{C}_{hs}, \Phi_{gc}\right) = T_3\left(p_c, p_e, T_1, \dot{m}, T_{hs,i}, \dot{C}_{hs}, \Phi_{gc}, HDF, \eta_{is}\right). \quad (13)$$

Both evaporation and heat transfer at IHX were assumed not-isobaric; the pressure losses dependencies for each processes can be easily inferred with expressions similar to equations (8) and (9).

The compressor isentropic and volumetric efficiency are expressed as linear functions of the pressure ratio and of the compressor model empirical constants, K_{is}, C_{is}, K_v and C_v:

$$\eta_{is} = C_{is} - K_{is}\frac{p_c}{p_e} = C_{is}\left(1 - \frac{K_{is}}{C_{is}}\frac{p_c}{p_e}\right), \quad (14)$$

$$\eta_v = C_v - K_v \frac{p_c}{p_e} = C_v \left(1 - \frac{K_v}{C_v} \frac{p_c}{p_e} \right). \tag{15}$$

Considering the compressor swept volume, $\dot{V}$, the refrigerant mass flow rate can be now written as:

$$\dot{m} = \dot{V} \cdot \eta_v \cdot \rho_1 = \dot{V} \cdot C_v \left(1 - \frac{K_v}{C_v} \frac{p_c}{p_e} \right) \cdot \rho_1 \left(p_e, T_1 \right). \tag{16}$$

Using equations (3-5) and (10-15) into equation (1) leads to:

$$COP = COP \left(p_c, \Delta T_{SH,e}, T_{hs,i}, T_{hsr,i}, \dot{C}_{hs}, \dot{C}_{hsr}, \Phi_{gc}, \Phi_e, \Phi_{ihx}, HDF, \dot{V}, K_{is}, K_v, C_{is}, C_v \right). \tag{17}$$

Equation (17) indicates that the system *COP* depends on the heat rejection pressure p_c, the evaporator superheat $\Delta T_{SH,e}$, on the gas cooler and evaporator secondary fluids heat capacity rates and inlet temperatures $\dot{C}_{hs}$, $\dot{C}_{hsr}$, $T_{hs,i}$, $T_{hsr,i}$. Moreover COP as expressed in equation (17) depends on the gas cooler, evaporator and IHX geometric characteristics Φ_{gc}, Φ_e, Φ_{ihx}, and on the compressor heat dissipation factor *HDF*, swept volume $\dot{V}$ and on the empirical constants K_{is}, C_{is}, K_v, C_v.

Please observe that the evaporator superheat can be reasonably considered an independent variable since in the most common carbon dioxide systems lay-out either a thermostatic expansion valve or a low pressure receiver are present.

Previous studies ([1], [6], [14]) show that there exists an optimal heat rejection pressure that gives a maximum *COP* for given values of the other variables. At the optimal heat rejection pressure $p_{c,opt}$, the partial derivative of the *COP* with respect to the heat rejection pressure should equal zero:

$$\left. \frac{\partial COP}{\partial p_c} \right|_{p_c = p_{c,opt}} = 0, \tag{18}$$

accordingly to equation (17), the following expression can thus be inferred for the exact solution to (18):

$$p_{c,opt} = p_{c,opt}\left(\Delta T_{SH,e}, T_{hs,i}, T_{hsr,i}, \dot{C}_{hs}, \dot{C}_{hsr}, \Phi_{gc}, \Phi_{e}, \Phi_{ihx}, HDF, \dot{V}, K_{is}, K_{v}, C_{is}, C_{v}\right). \quad (19)$$

Equation (18) shows the dependence of the optimal heat rejection pressure both on semi-empirical refrigerant reference equation of state [22] and on the heat transfer phenomena occurring in the heat exchangers.

2.2 Literature approximated methods

Several Authors, Liao et al. [17], Sarkar et al. [18], Kauf [16] and Chen and Gu [20] obtained numerical solutions to (18) and thus approximated polynomial expressions for the optimal gas cooler pressure. All of them, except Kauf [16], consider a single-stage refrigerating cycle working with an internal heat exchanger in their mathematical analysis. All the above expressions are based on several assumptions that differ one from another and also vary with the experimental behaviour of the facility. With respect to the former analysis, Liao et al. [17] transform the gas cooler outlet temperature, T_3 and the suction pressure and temperature, p_e and T_1, into independent variables, thus neglecting equations (12), (13) and (10). Moreover these Authors disregard the influence of the compressor volumetric efficiency and heat dissipation. The compressor efficiency influence is considered and equation (14) is introduced. Combining equations (1), (3), (4), (5) and (14) Liao et al. express the *COP* as:

$$COP = C_{is}\left(1 - \frac{K_{is}}{C_{is}}\frac{p_c}{p_e}\right)\frac{h_1(p_e,T_1) - h_3(p_c,T_3)}{h_{2s}(p_c,p_e,T_1) - h_1(p_e,T_1)}. \quad (20)$$

Equation (20) indicates that the system *COP* depends on the heat rejection pressure p_c, the suction pressure p_e, the suction temperature T_1, the gas cooler outlet temperature T_3, and the compressor empirical constants K_{is}, C_{is}:

$$COP = COP\left(p_c, p_e, T_1, T_3, K_{is}, C_{is}\right). \tag{21}$$

It can be pointed out that assuming gas cooler outlet temperature, suction pressure and temperature as independent variables caused the *COP* to be independent by the evaporator, gas cooler and IHX characteristics and by the heat exchangers secondary fluids thermo-physical properties and mass flow rates.

Equation (18) still defines the optimal heat rejection pressure. From equations (18) and (20), it can be inferred that the empirical constants K_{is} and C_{is} exert their influence on the optimal pressure in the form of $\frac{K_{is}}{C_{is}}$. Accordingly for the optimal value the following equation is proposed:

$$p_{c,Liao} = p_{c,Liao}\left(p_e, T_1, T_3, \frac{K_{is}}{C_{is}}\right). \tag{22}$$

The Authors suggest the following approximate thermodynamic expression of equation (22) neglecting the influence of suction temperature, T_1, and considering the refrigerant biunique relation between suction pressure, p_e, and refrigerant dew point evaporation temperature, T_e:

$$p_{c,Liao} = \frac{2.7572 + 0.1304 \cdot T_e - 3.072 \cdot \frac{K_{is}}{C_{is}}}{1 + 0.0538 \cdot T_e + 0.1606 \cdot \frac{K_{is}}{C_{is}}} \cdot T_3 - \frac{8.7946 + 0.02605 \cdot T_e - 105.48 \cdot \frac{K_{is}}{C_{is}}}{1 + 0.05163 \cdot T_e + 0.2212 \cdot \frac{K_{is}}{C_{is}}}. \tag{23}$$

Since Liao et al. [17] solved the problem of optimising equation (21), which domain is constrained by equations (10, 12 and 13), in the unconstrained

domain of the thermodynamic variables T_3 and p_e, the proposed approximated solution can't be considered an optimal one for the constrained function. Furthermore, if the approximated solution is implemented on board of a real unit control system, the gas cooler outlet temperature and evaporation temperature can't be considered as independent variables. Considering equations (3-5) and (10-15) and applying Liao et al. [17] equation, the system working pressure value is determined solving the following system of equations:

$$\begin{cases} p_{c,Liao} = \dfrac{2.7572 + 0.1304 \cdot T_{e,Liao} - 3.072 \cdot \dfrac{K_{is}}{C_{is}}}{1 + 0.0538 \cdot T_{e,Liao} + 0.1606 \cdot \dfrac{K_{is}}{C_{is}}} \cdot T_{3,Liao} + \ldots \\ \ldots - \dfrac{8.7946 + 0.02605 \cdot T_{e,Liao} - 105.48 \cdot \dfrac{K_{is}}{C_{is}}}{1 + 0.05163 \cdot T_{e,Liao} + 0.2212 \cdot \dfrac{K_{is}}{C_{is}}} \\ T_{3,Liao} = T_3\left(p_{c,Liao}, \Delta T_{SH,e}, T_{hs,i}, T_{hsr,i}, \dot{C}_{hs}, \dot{C}_{hsr}, \Phi_{gc}, \Phi_e, \Phi_{ihx}, HDF, \dot{V}, K_{is}, K_v, C_{is}, C_v\right) \\ p_{e,Liao} = p_e\left(p_{c,Liao}, \Delta T_{SH,e}, T_{hs,i}, T_{hsr,i}, \dot{C}_{hs}, \dot{C}_{hsr}, \Phi_{gc}, \Phi_e, \Phi_{ihx}, HDF, \dot{V}, K_{is}, K_v, C_{is}, C_v\right) \\ T_{e,Liao} = T_e\left(p_{e,Liao}\right) \end{cases} . \quad (24)$$

Sarkar et al. [18] make a similar analysis but they neglect the influence of the compressor characteristic $\frac{K_{is}}{C_{is}}$ ratio in the determination of their approximated expression for equation (22):

$$p_{c,Sarkar} = 4.9 + 2.256 \cdot T_3 - 0.17 \cdot T_e + 0.002 \cdot T_3^2 . \quad (25)$$

The real system working pressure is obtained substituting equation (25) approximated solution for Liao's expression in system (24) and solving it.

On similar assumptions, Chen and Gu [20] propose a thermodynamic approximate expression of the optimal high pressure problem. These Authors

ignore the effect of suction pressure but keep the suction temperature, T_1, as a dependent variable. In fact, the IHX efficiency is defined:

$$\varepsilon_{ihx} = \frac{h_1 - h_{1'}}{\min\left\{\left[h(p_e, T_3) - h_{1'}\right], \left[h_3 - h(p_c, T_{1'})\right]\right\}}, \tag{26}$$

and equation (10) replaced by:

$$T_1 = T_1\left(p_c, p_e, T_3, x_{e,o}, \dot{m}, \varepsilon_{ihx}\right), \tag{27}$$

where the evaporator outlet quality, $x_{e,o}$, replaces the evaporator superheat, $\Delta T_{SH,e}$, variable, considering Chen and Gu's system lay-out. Furthermore, the gas cooler outlet temperature, T_3, is expressed as a function of the heat sink fluid temperature, and equation (13) is substituted by the following:

$$T_3 = -0.0015269 \cdot T_{hs,i}^2 - 0.028866 \cdot T_{hs,i} + 7.7126. \tag{28}$$

As Sarkar et al. [18], Chen and Gu [20] ignore the influence of the compressor characteristic $\frac{K_{is}}{C_{is}}$ ratio in the determination of optimal pressure, obtaining:

$$p_{c,Chen} = A\left(\varepsilon_{ixh}, x_{e,o}\right) \cdot T_{hs,i} + B\left(\varepsilon_{ixh}, x_{e,o}\right), \tag{29}$$

which, considering null IHX efficiency and saturated vapour at the evaporator outlet, gives:

$$p_{c,Chen} = 2.304 \cdot T_{hs,i} + 19.29. \tag{30}$$

Kauf [16] doesn't approach the problem only from a thermodynamic point of view but simulates the system cycle introducing heat exchangers efficiency. For the gas cooler, the Author gives the following efficiency definition:

$$\varepsilon_{gc} = \frac{T_{2d} - T_3}{T_{2d} - T_{hs,i}}. \tag{31}$$

So instead of equation (13), the following can be written:

$$T_3 = T_{2d} - \left(T_{2d} - T_{hs,i}\right) \cdot \varepsilon_{gc}, \tag{32}$$

which the Author, considering a constant gas cooler efficiency, reduces to:

$$T_3 \approx T_{hs,i} + 2.9 \,. \tag{33}$$

For the evaporator, Kauf introduces the following efficiency definition:

$$\varepsilon_e = \frac{T_{hsr,i} - T_{hsr,o}}{T_{hsr,i} - T_e} \,. \tag{34}$$

So instead of equation (12), the following can be written:

$$p_e = p_e\left(\varepsilon_e, T_{hsr,i}, T_{hsr,o}\right) \,. \tag{35}$$

As the analysed system has no IHX, considering (33) and (35), equation (17) can be written as:

$$COP = COP\left(p_c, \Delta T_{SH,e}, T_{hs,i}, T_{hsr,i}, T_{hsr,o}, \varepsilon_e, HDF, \dot{V}, K_{is}, K_v, C_{is}, C_v\right). \tag{36}$$

In the determination of the approximated solution to equation (18), Kauf [16] neglects the influence of the compressor swept volume, heat dissipation factor and efficiency parameters. Furthermore the influence on the optimal high cycle pressure of the evaporator efficiency, superheat and secondary fluid temperature and mass flow rate is ignored. The approximated solution to equation (18) is thus expressed in this simple form:

$$p_{c,Kauf} = 2.6 \cdot T_{hs,i} \,. \tag{37}$$

In the derivation of the previous approximated solutions to equation (18), all the Authors made different simplifying assumptions concerning the independent variables present in the functional form of the exact problem solution (19), that can be summarised as follows:

1) completely neglecting the influence of one or more variables, as for example all the Authors did with the compression swept volume, $\dot{V}$;
2) to remove the dependency of some refrigerant thermodynamic variable on one or more of the independent variables in order to solve the problem on a

thermodynamic basis, i.e. Liao et al. [17] considered the gas cooler outlet temperature as an independent variable and ignored its dependency on the cycle high pressure, the gas cooler geometric characteristic and other variables (see equation (13));

3) to introduce empirical correlations instead of equations (10-13) in order to make the problem dependent only on refrigerant thermodynamic variables, for example Chen and Gu [20] related the gas cooler outlet temperature to the heat sink fluid temperature (see equation (28)).

The first kind of hypothesis must be in general verified. Depending on the considered application and working conditions, the resulting approximated solution could be sufficiently close to the exact one or not. The second kind of hypothesis could lead to misleading approximated solutions because they are obtained removing some constraints to the optimisation problem. Finally the use of empirical correlations instead of equations (10-13) might be an acceptable assumption, provided that the most important functional dependencies are maintained. For example Chen and Gu [20] related the gas cooler outlet temperature to the heat sink fluid temperature but not to cycle high pressure nor to the gas cooler geometry or to the secondary fluid heat capacity rate. Changing the gas cooler heat transfer surface would result in a different empirical correlation, and thus in a new approximated solution to the pressure problem.

Different applications are simulated in the following to compare the deviations of the analysed approximated expressions to the numerical solutions and the effect of these deviations on the COP. In Section 4 only the dependencies of the optimal pressure from the gas cooler secondary fluid heat capacity rate and temperature, from the gas cooler geometric characteristics and from the

compressor empirical constants, K_{is}, C_{is}, are analysed. In Section 5 a commercial refrigeration plant and heat pump water heater are analysed under different working conditions and optimal pressures are matched up to the approximated expressions.

3. Heat exchangers and system modelling

For the numerical solution of heat exchangers and refrigeration systems, a Finite Volume (FVM) based model was adopted. In the code heat exchangers are defined by their geometrical parameters and the phenomenological coefficients which characterise heat transfer and pressure drops are evaluated according to common correlations reported in open literature (see Table 1). For a complete vapour compression system, comprising an evaporator, a gas cooler, an internal heat exchanger and a compressor, the governing equations of each component (for the compressor a simple lumped parameter model based on equations (14) and (15) was adopted) can be reduced to this general form:

$$f\left(p_i, p_o, h_i, h_o, \dot{m}\right) = 0. \tag{38}$$

Therefore, the problem is reduced to calculate the solution to a non-linear system of equations written in equation (38) form. The system of equations is solved using Powell's hybrid algorithm [30]. More details about the numerical models and their validation are reported in [31], [13], Zilio et al. [32], Cavallini et al. [33]. The finned coil gas cooler model considered the heat conduction phenomena through fins as detailed in Singh et al. [34].

4. The effect of the outlet gas cooler temperature simplifying assumptions on optimal pressure determination

In this section the dependencies of the optimal pressure on the gas cooler secondary fluid heat capacity rate and inlet temperature and on the gas cooler geometric characteristics are analysed. Several finned coil air cooled and coaxial water cooled heat exchangers were simulated. The influence of suction temperature, IHX outlet enthalpy, suction pressure, heat dissipation factor and compressor volumetric efficiency on the optimal pressure was not considered. These variables are kept constant in the simulation as specified in Table 2 for finned coil and coaxial gas coolers. Liao's compressor isentropic efficiency equation is assumed. Tables 3 reports the baseline simulated finned coil gas cooler "A" geometric characteristics, "B" and "C" heat exchangers are obtained from the baseline one reducing by 56% tube length and air mass flow rate respectively.

Tables 4 reports the baseline simulated coaxial gas cooler "A" geometric characteristics, "B" and "C" heat exchangers are obtained from the baseline one varying by +18% and -26% water mass flow rate respectively.

In the considered hypothesis, all the heat exchangers were simulated to find the numerical solution to equation (19) under different heat sink fluid inlet temperature. For the finned coil, air inlet temperature was varied from 25 ℃ to 40 ℃, while water inlet temperature of the coaxial heat exchangers ranged from 10 ℃ to 35 ℃. In Table 5 and 6 the optimal pressu re and efficiency results are matched up to those obtained with the approximated solutions presented in Section 2 for finned coils and coaxial heat exchanger respectively. Optimal pressure (Δp_c) and COP (ΔCOP) deviations of the authors' expressions are

reported. Each approximated solution is applied only within the validity range suggested by its authors. From the comparison presented in Table 5 and 6, it can be observed that the solutions that best fit the optimal one are those of Liao and Sarkar.

As explained in Section 2, these authors considered gas cooler outlet temperature T_3 as an independent variable in the determination of their approximated solutions. The dependency of this variable on the cycle high pressure and secondary fluid inlet temperature, which is expressed by equation (13), is instead evident in Figure 3 in the case of baseline coaxial heat exchanger ("A" configuration in Table 4). In the mentioned example, the strong dependence of T_3 from p_c is related to the specific heat exchanger geometric characteristics and secondary fluid heat capacity rate and temperature. If the gas cooler outlet refrigerant thermodynamic state happens to be in the pseudo-critical region, T_3 reaches its maximum value, because of the sudden increase in the CO_2 isobaric heat capacity. T_3 becomes almost independent from p_c when the slope of the isotherm curves in the thermodynamic p-h diagram result near vertical. In Figure 3 the optimal high pressure value curve is also plotted together with Liao and Sarkar approximated solution pressure curves showing significant deviations up to -10 10^5 Pa. The corresponding COP trends are reported in Figure 4, the maximum COP deviation is -5.4% and occurs at 15 ℃.

In the case of the finned coil baseline gascooler ("A" configuration in Table 3), gas cooler outlet temperature happens not to be much influenced by gas cooler pressure, thus better fitting to the Liao and Sarkar simplifying hypothesis and resulting in limited Liao and Sarkar COP deviations from the optimal one (Table 5).

To obtain their approximated solution, Kauf and Chen and Gu substitute equation (13) for an equation correlating gas cooler outlet temperature only with heat sink fluid inlet temperature (see equations (28) and (33)). The dependency of this variable on the gas cooler heat transfer area and secondary fluid heat capacity rate is clearly pointed out in Figure 5. The refrigerant gas cooler outlet temperature is plotted against secondary fluid inlet temperature for the different considered finned coil heat exchangers at different pressures. Kauf and Chen and Gu trends don't match the operating curves of the different simulated heat exchangers which are affected by heat exchange area, air flow rate and operating pressure. Analysing Table 5 and 6 data, it appears that approximated solutions adopting *a priori* gas cooler outlet temperature equations based on secondary fluid temperature behaves worse than solutions obtained with the independent variable refrigerant outlet temperature hypothesis. If the *a priori* correlations implemented in the machine controller are far from the gas cooler real behaviour, the efficiency will be far lower than the optimal one. Compare for example Figure 5 trends of "A" unit with Chen and Gu equation, in this case the COP penalisation reaches 9%. Instead when Liao or Sarkar's solution are implemented on board of a real unit control system, the operating pressure value is determined solving system (24). In particular Liao's high pressure is determined by the measured gas cooler outlet temperature, which is obviously influenced by heat sink fluid temperature but also by its capacity rate and by the heat exchanger geometry (see the second equation in system (24)). This is clearly pointed out in Figure 3, where for each water inlet temperature, the working condition of a unit controlled by Liao's equation is determined by the intersection between Liao's equation curve and the gas cooler operating outlet temperature profile.

5. Approximated optimal pressure solutions applied to commercial refrigeration plants and heat pump water heaters

In the analysis of different carbon dioxide vapour compression systems, some of the hypotheses of Section 4 must be evaluated in order to correctly solve the high pressure optimisation problem. In particular the following assumptions should be certainly discussed:

1) constant gas cooler heat sink fluid mass flow rate;
2) the compression swept volume, $\dot{V}$, is an independent variable.

To this regard, the following CO_2 applications will be analysed:

a) *Medium temperature direct expansion multi-compressor commercial refrigeration plant with air cooled condensers* (Figure 6). The system is equipped with an intermediate pressure receiver (4), to manage the seasonal and load associated charge variations. In transcritical operation, the gas cooler air flow rate is kept constant. Instead the compressors are alternatively switched on and off in order to keep the evaporation pressure close to a set-point value when the cooling load varies. A relation between the cooling load and the swept volume must be introduced for the problem solution;

b) *Heat pump water heater with supply water temperature control varying the water mass flow rate* (Figure 7). The system is equipped with a low pressure receiver (5), to manage the seasonal and load associated charge variations. The heat sink fluid flow rate is intrinsically variable while the compression swept volume is constant. A relation between the

outlet water temperature set-point and the water mass flow rate must be introduced for the problem solution.

5.1. Commercial refrigeration unit

For the commercial refrigeration system, relations (3-5) and (10-15) are still valid but the following expression for the swept volume, $\dot{V}$, as function of the cooling load, Q, can be written:

$$\dot{V} = \frac{Q}{\eta_v \cdot \rho_1} \cdot \frac{1}{(h_1 - h_3)} = \dot{V}\left(p_c, \Delta T_{SH,e}, T_{hs,i}, T_{hsr,i}, \dot{C}_{hs}, \dot{C}_{hsr}, \Phi_{gc}, \Phi_e, \Phi_{ihx}, HDF, K_{is}, K_v, C_{is}, C_v, Q\right) \quad (39)$$

.

The introduction of equation (39) in equations (17), (19) and in system (24), points out the dependency on the system cooling load, and not more on the compression swept volume, of both the exact optimal pressure problem solution and of Liao et al. [17] and Sarkar et al. [18] approximated equations.

The system was simulated at constant evaporation pressure with the operating conditions specified in Table 7. The system was equipped with the baseline “A” finned coiled gas cooler of Table 3. Compressor isentropic and volumetric efficiency equations of Table 7 were obtained from the results presented in Bernabei et al. [10]. Four compressor volumetric capacity steps were simulated. In Table 8 the optimal pressure and efficiency results are matched up to those obtained with the approximated solutions. Optimal pressure (Δp_c) and COP (ΔCOP) deviations of the authors’ expressions are reported. This case differs from the ones presented in Section 4 because:

a) the volumetric and isentropic compressor efficiency are representative of the performance of real compressors;

b) the effect of different compressors capacity is considered for a specific gas cooler.

Considering full load conditions, again Liao and Sarkar's equations give better performances than Chen and Gu correlation. In this case Kauf high pressure is close to the optimal value in its range of validity. The effects of the plant cooling capacity control are pointed out in Figure 8, where the optimal high cycle pressure is compared to the Authors correlations for 25% and 100% compressor volumetric capacity. With the exception of Chen and Gu correlation, all other approximated solutions give a maximum pressure deviation of 4.3 10^5 Pa and COP deviation of -2.1%.

5.2. Heat pump water heater

For the heat pump water heater, relations (3-5) and (10-15) are still valid but the following expression for the gas cooler secondary fluid heat capacity rate, $\dot{C}_{hs}$, as function of its outlet water temperature set-point, $T_{hs,o}$, can be written:

$$\dot{C}_{hs} = \frac{\eta_v \cdot \rho_1 \cdot \dot{V} \cdot (h_{2''} - h_3)}{T_{hs,o} - T_{hs,i}} = \dot{C}_{hs}\left(p_c, \Delta T_{SH,e}, T_{hs,i}, T_{hs,o}, T_{hsr,i}, \dot{C}_{hsr}, \Phi_{gc}, \Phi_e, \Phi_{ihx}, HDF, \dot{V}, K_{is}, K_v, C_{is}, C_v\right). \quad (40)$$

This correlation is the consequence of the control system that fixes the hot water temperature at the set-point value. The introduction of equation (40) in equations (17), (19) and in system (24), points out the dependency on the gas cooler water outlet set-point temperature, and no more on the water mass flow rate, of both the exact optimal pressure problem solution and of Liao et al. [17] and Sarkar et al. [18] approximated solutions.

The system was simulated at constant water outlet temperature with the operating conditions specified in Table 7. The system was equipped with the

baseline “A” coaxial gas cooler of Table 4. Compressor isentropic and volumetric efficiency equations of Table 7 were obtained from the results presented in [11]. The simulations were carried out for two different water inlet temperature values and four evaporator air inlet temperatures with a relative humidity equal to 80%. The main characteristics of the finned-coil evaporator and of the coaxial IHX that were used in the simulations are summarised in Table 9. In Table 10 the optimal pressure and efficiency results are matched up to those obtained with Liao and Sarkar’s solutions with respect to a water set point value of 60 °C. The other correlations were not applicable in their range of validity. Optimal pressure (Δp_c) and COP (ΔCOP) deviations of the authors’ expressions are reported. For a unit with outlet water temperature control actuated varying its mass flow rate, the results clearly point out that the approximated solutions high pressure values are far from the optimal ones. Pressure deviations are up to of -12.5 10^5 Pa and COP deviations ranging from 10.3% up to 30.1%. The behaviour of the heat pump controlled by Liao’s equation is pointed out in Figure 9. Water and refrigerant gas cooler outlet temperature and COP are plotted as a function of high cycle pressure and water mass flow rate at 20 °C external air temperature and 15 °C gas cooler water inlet temperature. In the graphs, the unit operating points *locus* is indicated by shadowed grey lines. Liao’s control law crosses this line in correspondence of 84.0 10^5 Pa. For this pressure the water mass flow rate is very low in order to keep constant the 60 °C water set point value, greatly reducing the gas cooler efficiency. This result in a high refrigerant gas cooler outlet temperature and, consequently low COP value, observed in Figure 9 in correspondence of Liao’s operating conditions (full circle markers).

6. Conclusions

In this work the optimal energy efficiency and high cycle pressure problem of single stage refrigerating vapour compressor units operating with carbon dioxide as refrigerant in a transcritical cycle was addressed. Literature approximated solutions to the optimisation problem were questioned and critically discussed. The analysis of different gas coolers pointed the strong sensitivity of the refrigerant outlet temperature not only from the secondary fluid temperature but also from its capacity rate and from the heat exchanger geometric characteristics. Nevertheless it resulted that approximated solutions obtained considering the carbon dioxide gas cooler outlet temperature as an independent variable behaves better than solutions correlating it to secondary fluid inlet temperature. The analysed finned coil gas coolers, under the assumption of constant suction conditions, compressor mass flow rate and at different heat capacity rates and temperatures of the inlet air, showed a COP maximum deviation of -3% with respect to the optimal one, when using correlations that consider the gas cooler outlet temperature as an independent variable, and -22% with those correlating it to the air inlet temperature. The same analysis, under similar assumptions, was extended to coaxial heat exchangers, showing –6.3% and –20.6% maximum deviations respectively, due to the stronger dependency of the gas cooler outlet temperature on the gas cooler pressure. The simulation of a commercial refrigeration plant with compressor cooling capacity control showed similar performance of the considered approximated solutions with respect to the optimal one (maximum deviation was –5.6%). Finally a heat pump water heater with supply water temperature control varying its mass flow rate pointed out large energy penalisation of all the literature solutions, up to -30.1%. It can be concluded that

an approximated correlation must be critically evaluated before implementing it in a real controller. The underlying simplifying hypotheses can be acceptable or not, depending on the considered application, its design, heat sink fluid heat capacity and temperature level, and finally on its control system. The control of a refrigeration system based on a priori solutions is, indeed, a critical issue. Controllers presently employed on the market are based on a PID feedback loop that aims at tracking a reference set-point generated by an approximated equation. This can eventually configure an adaptive control architecture but, being the solution not the optimal one, the system overall energy efficiency is penalised. This control technique might be efficiently used only if the implemented approximated solution is obtained by considering the operating characteristics of the specific refrigeration unit. In order to obtain such a tailored equation, an experimental or simulation campaign is needed for each unit, thus requiring dedicated tuning for each controller. A more efficient solution requires the implementation of a real-time algorithm for determining the optimal (or quasi-optimal) pressure value in the constrained domain of the independent variables. A viable solution to this optimisation problem could be provided by computational intelligence algorithms.

REFERENCES

[1] Lorentzen G, 1994. Revival of carbon dioxide as a refrigerant. Int. J. Refrig. 17, 292-301.

[2] Cavallini A, Nekså P., 2001. Prospects for the return of CO_2 as a refrigerant. Proceedings VI° Congreso Iberoamericano de Aire Aco ndicionado y Refrigeración , CIAR, Buenos Aires, Argentina; 761-790.

[3] Nekså P, 2002. CO_2 heat pump systems. Int. J. Refrigeration, 25(4), 421-427.

[4] Groll E.A., 2001. Review of recent research on the use of CO_2 for air conditioning and refrigeration. Proceedings Clima 2000, Napoli, Italy.

[5] Cecchinato L., Corradi M., Fornasieri E., Minetto S., Stringari P., Zilio C., 2009. Thermodynamic analysis of different two-stage transcritical carbon dioxide cycles. Int. J. Refrig. 32, 1058-1067.

[6] Kim M.H., Pettersen J., Bullard C.W., 2004. Fundamental process and system design issues in CO_2 vapour compression systems. Progress in Energy and Combustion Science 30(2), 1119-1174.

[7] Brown J.S., Yana-Motta S.F., Domanski P.A., 2002. Comparative analysis of an automotive air conditioning systems operating with CO_2 and R134a, Int. J. Refrig 25, 19–32.

[8] Liu H., Chen J., Chen Z., 2005. Experimental investigation of a CO_2 automotive air conditioner. Int. J. Refrig. 28, 1293–1301.

[9] Girotto S., Minetto S., Nekså P., 2004. Commercial refrigeration system using CO_2 as the refrigerant. Int. J. Refrig. 27, 717–723.

[10] Bernabei M., Cecchinato L., Chiarello M., Fornasieri E., 2008. Design and experimental analysis of a carbon dioxide transcritical chiller for commercial

refrigeration. 8th IIR Gustav Lorentzen Conf. on Natural Working Fluids, Copenhagen, Denmark, 7-10 September, 295-302.

[11] Fornasieri E., Girotto S., Minetto S., 2008. CO_2 heat pump for domestic hot water. 8th IIR Gustav Lorentzen Conf. on Natural Working Fluids, Copenhagen, 7-10 September, 545-552.

[12] Nekså, P., Rekstad, H., Zakeri, G.R. and Schiefloe, P.A., 1998. CO_2 - heat pump water heater: characteristics, system design and experimental results. Int. J. Refrig. 21, 172-179.

[13] Cecchinato L., Corradi M., Fornasieri E., Zamboni L., 2005. Carbon dioxide as refrigerant for tap water heat pumps: A comparison with the traditional solution. Int. J. Refrig. 28, 1250–1258.

[14] Casson V., Cecchinato L., Corradi M., Fornasieri E., Girotto S., Minetto S., Zamboni L., Zilio C., 2003. Optimisation of the throttling system in a CO_2 refrigerating machine. Int. J. Refrig. 26, 926–935.

[15] Inokuty H., 1923. Approximate graphical method of finding compression pressure of CO_2 refrigerant machine for max. coefficient of performance. 92th Japan Society of Mechanical Engineers, March 8.

[16] Kauf F., 1999. Determination of the optimum high pressure for transcritical CO_2 refrigeration cycles. Int. J. Therm. Sci. 38, 325–330.

[17] Liao S.M., Zhao T.S., Jakobsen A., 2000. A correlation of optimal heat rejection pressures in transcritical carbon dioxide cycles. Appl. Therm. Eng. 20, 831–841.

[18] Sarkar J., Bhattacharyya S., Ram Gopal M., 2004. Optimisation of a transcritical CO_2 heat pump cycle for simultaneous cooling and heating applications, Int. J. Refrig. 27, 830–838.

[19] Sarkar J., Bhattacharyya S., Ram Gopal M., 2007. Natural refrigerant-based subcritical and transcritical cycles for high temperature heating, Int. J. Refrig. 30, 3–10.

[20] Chen Y., Gu J., 2005. The optimum high pressure for CO_2 transcritical refrigeration systems with internal heat exchangers. Int. J. Refrig. 28, 1238–1249.

[21] Cabello R., Sanchez D., Llopis R., Torrella E., 2008. Experimental evaluation of the energy efficiency of a CO_2 refrigerating plant working in transcritical conditions. Appl. Therm. Eng. 28, 1596–1604.

[22] Span R., Wagner W., 1996. A New Equation of State for Carbon Dioxide Covering the Fluid Region from the Triple-Point Temperature to 1100 K at Pressures up to 800 MPa. J. Phys. Chem. Ref. Data 25(6),1509-1596.

[23] Wang C., Chi K., Chang C., 2000. Heat transfer and friction characteristics of plain fin-and-tube heat exchangers. Int. J. of Heat and Mass Transfer 43, 2693-2700.

[24] Idelchik E., 1994. Handbook of Hydraulic Resistance. 3rd Edition, CRC Press.

[25] Gnielinski V., 1976. New equations for heat and mass transfer in turbulent pipe and channel flow. Int. Chem. Eng. 16, 359-368.

[26] Churchill S. W., 1977. Friction-factor equation spans all fluid flow regimes. Chem. Eng. 7, 91-92, 1977.

[27] Dang C., Hihara E., 2004, In-tube cooling heat transfer of supercritical carbon dioxide. Part 1. Experimental measurement. Int. J. Refrig. 27, 736-747.

[28] Cheng L., Ribatski G., Wojtan L., Thome J.R., 2006. New Flow Boiling Heat Transfer Model and Flow Pattern Map for Carbon Dioxide Evaporating inside Tubes. Int. J. Heat and Mass Transfer 49, 4082–4094.

[29] Friedel L., 1979. Improved friction pressure drop for horizontal and vertical two-phase pipe flow. Europ. Two-phase flow group meet, Paper E2., Ispra.

[30] Powell M.J.D., 1977. Restart procedures for the conjugate gradient method. Mathematical Programming 12, 241-254.

[31] Casson V., Cecchinato L., Del Col D., Fornasieri E., Zilio C.,2002. An innovative model for the simulation of a finned coil evaporator. Proc. 12th Heat Transfer Conference, 285-290.

[32] Zilio C., Cecchinato L., Corradi M., Schiochet G., 2007. An assessment of heat transfer through fins in a fin-and-tube gas cooler for transcritical carbon dioxide cycles, HVAC&R Research 13(3), 457-470.

[33] Cavallini A, Chiarello M., Fornasieri E., Zilio C., 2008. Experimental Analysis of Carbon Dioxide Coiled Evaporators. 8th IIR Gustav Lorentzen Conf. on Natural Working Fluids, Copenhagen, Denmark, 7-10 September, 334-341.

[34] Singh V., Aute V., Radermacher R., 2008. Numerical approach for modeling air-to-refrigerant fin-and-tube heat exchanger with tube-to-tube heat transfer. Int. J. of Refrig. 31,1414-1425.

FIGURES

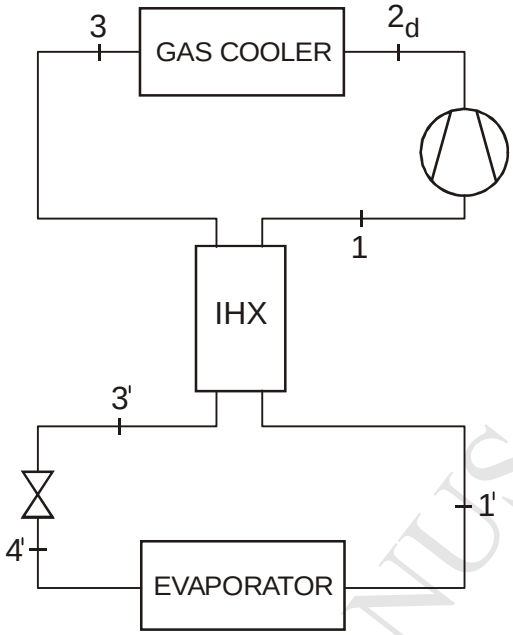

Fig. 1.

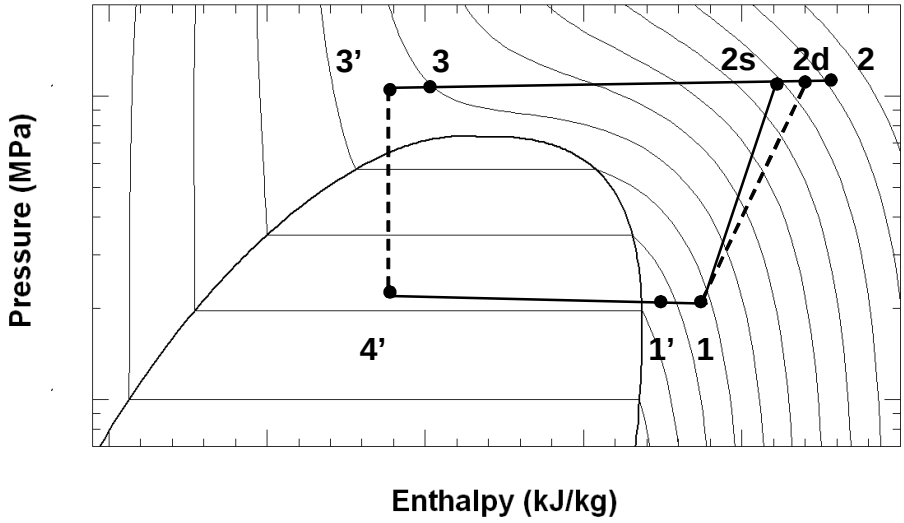

Fig. 2.

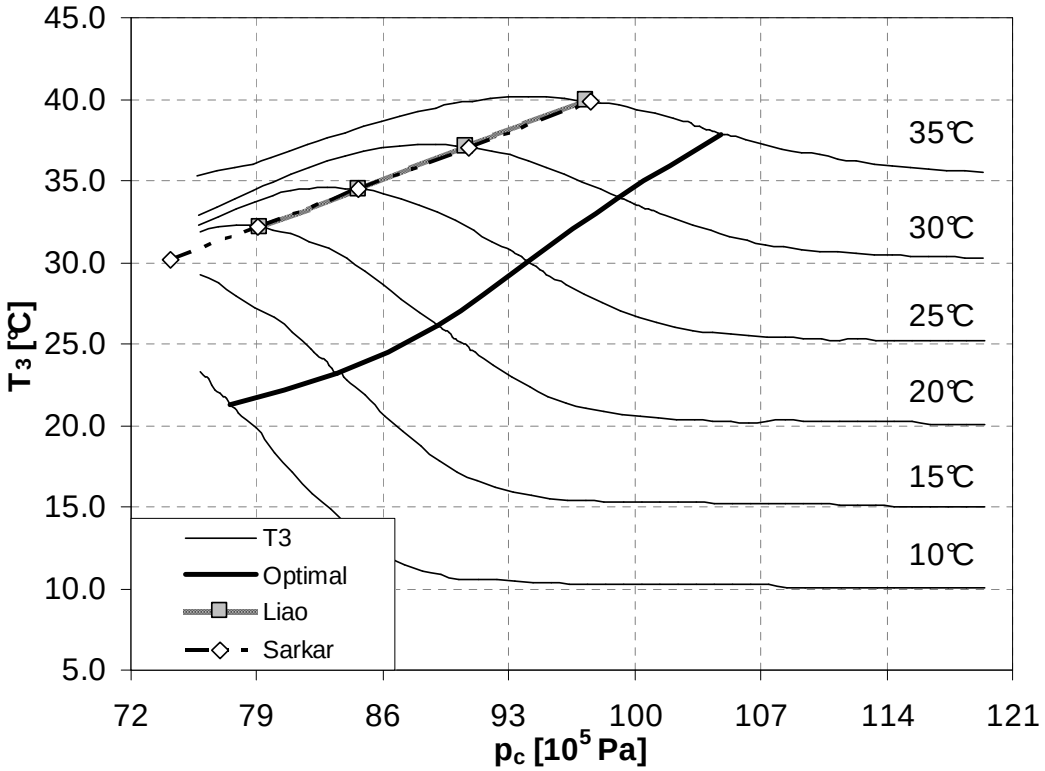

Fig. 3.

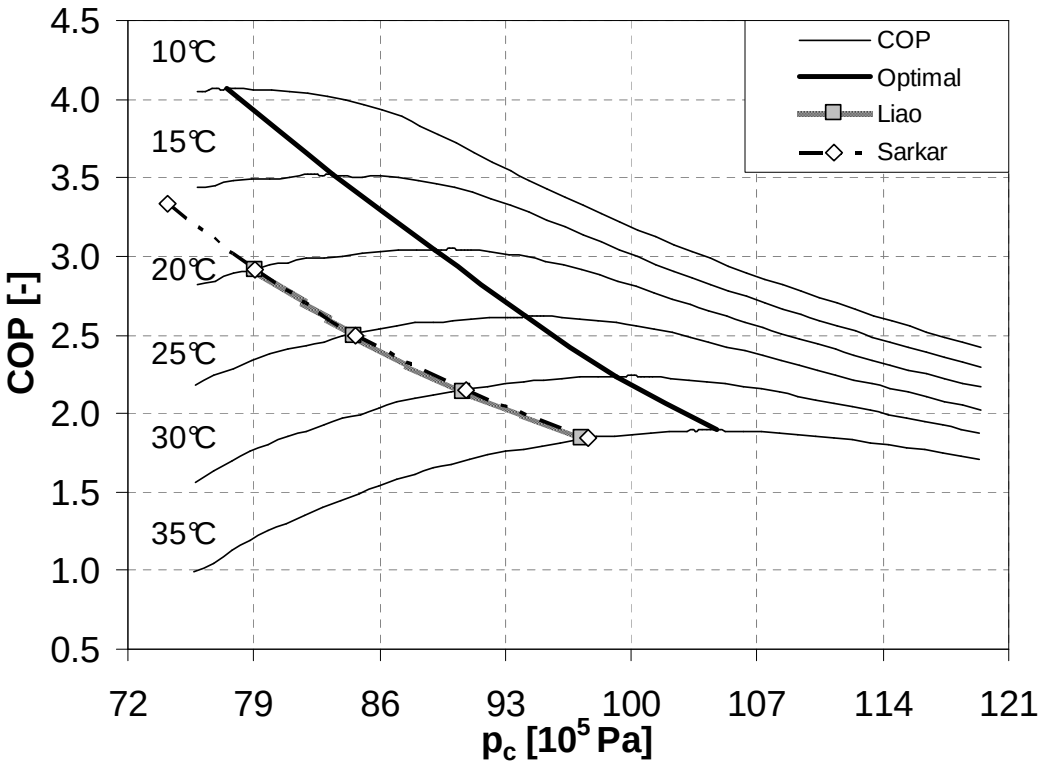

Fig 4.

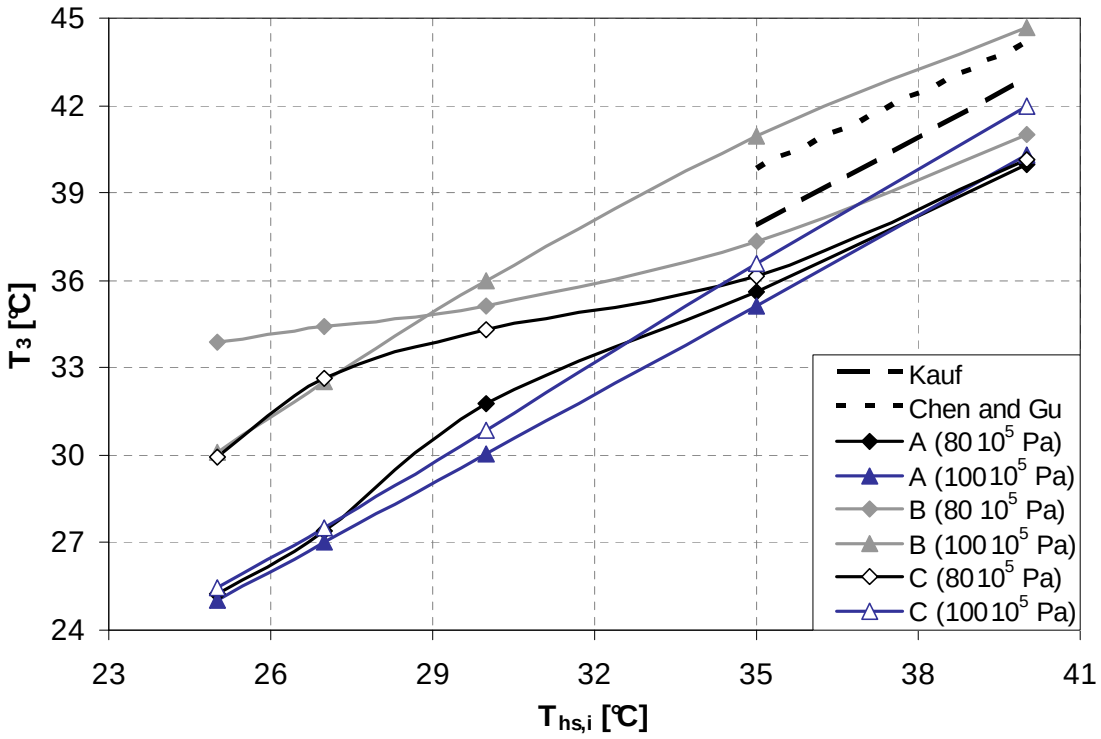

Fig 5.

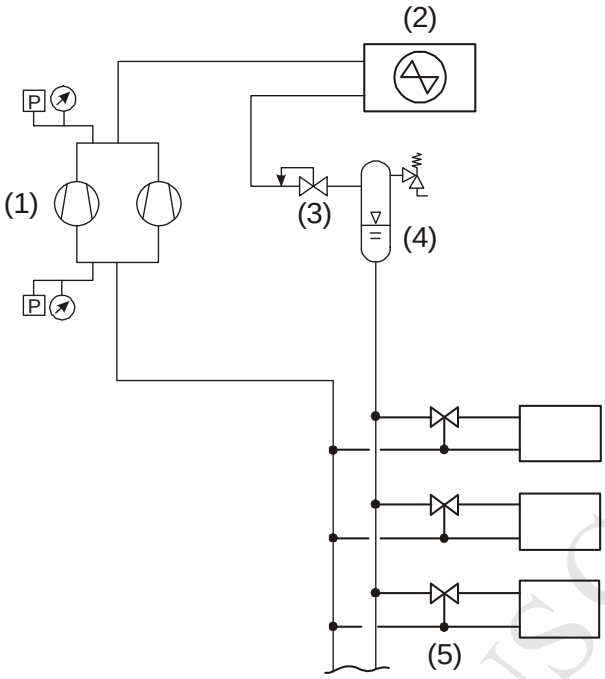

Fig. 6.

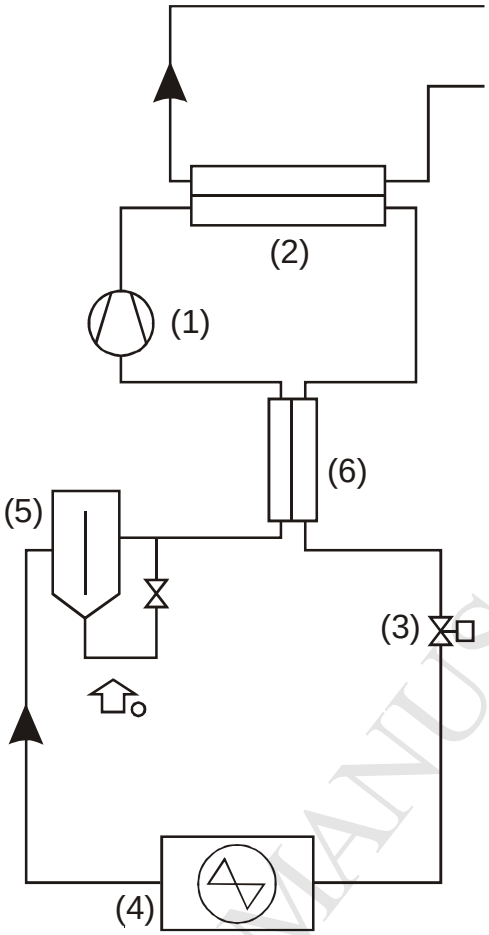

Fig. 7.

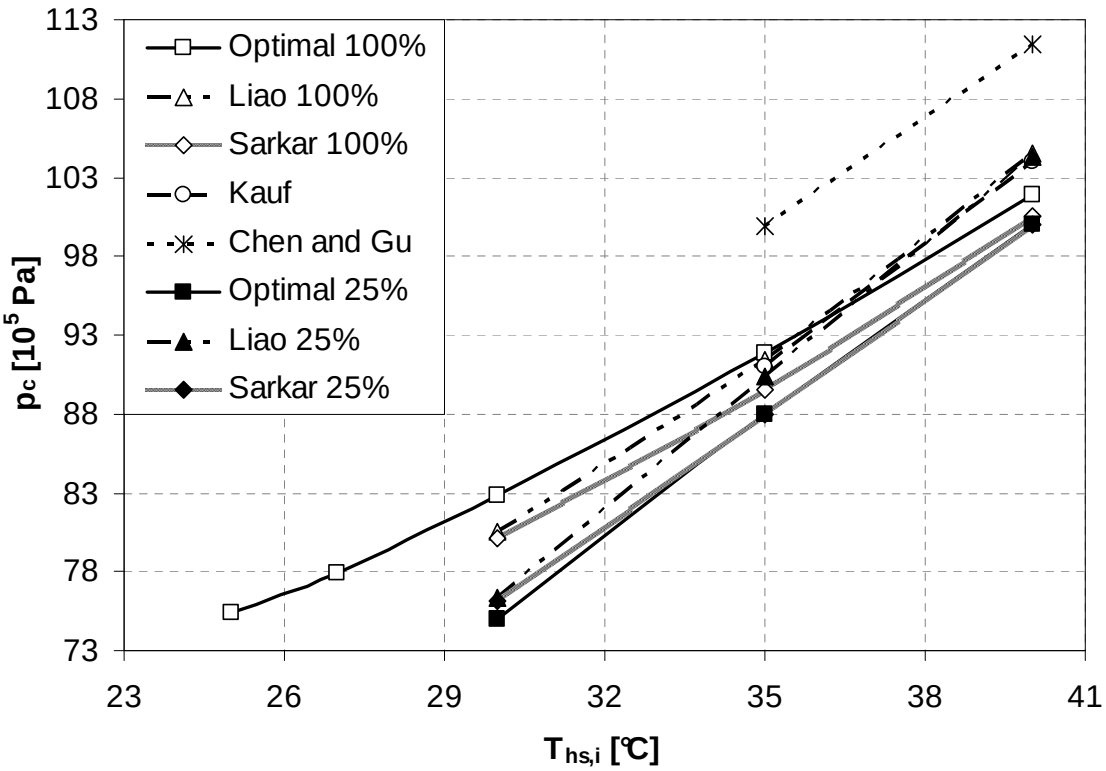

Fig 8.

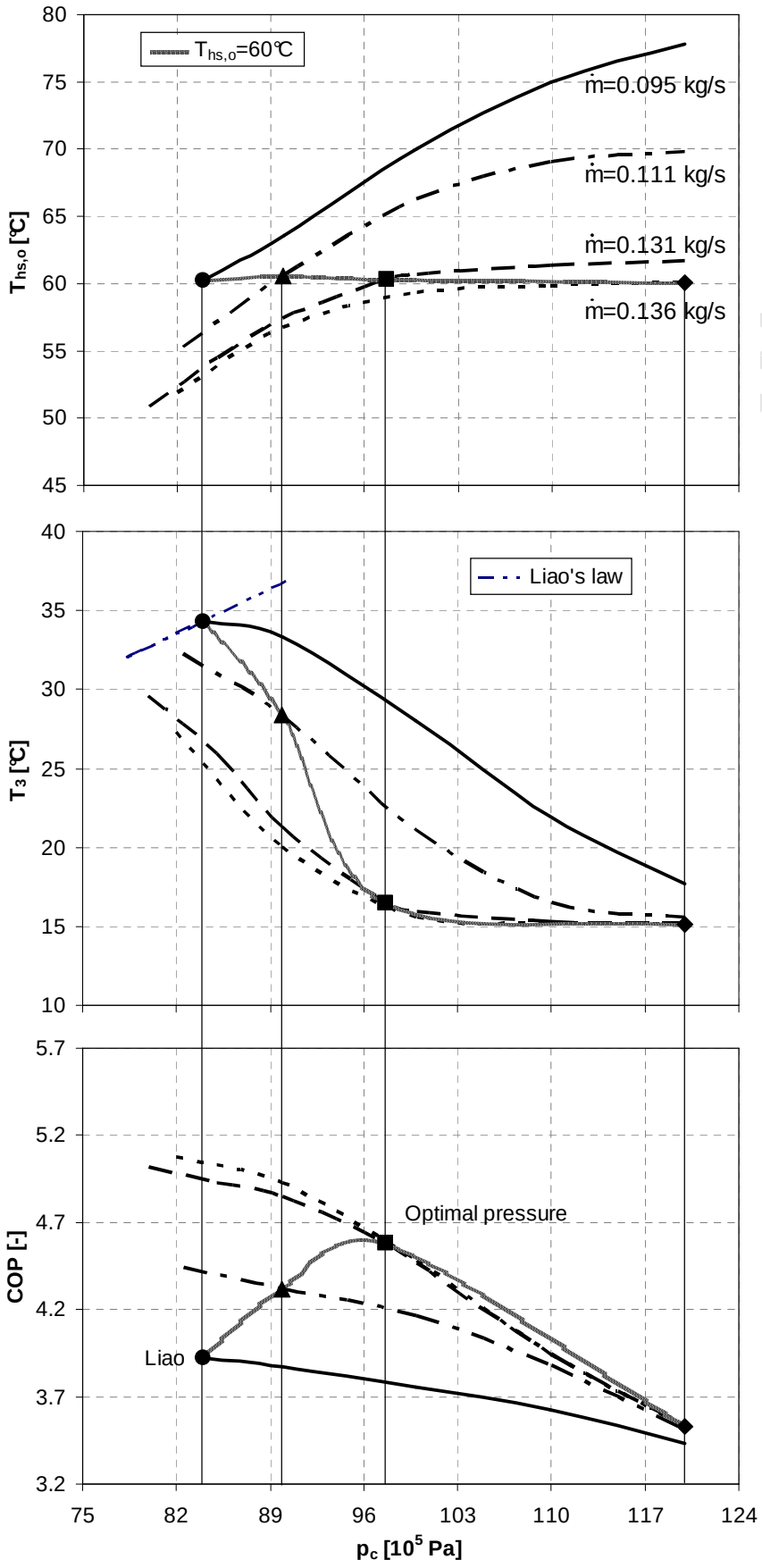
$T_{hs,o}$=60℃
ṁ=0.095 kg/s
ṁ=0.111 kg/s
ṁ=0.131 kg/s
ṁ=0.136 kg/s
$T_{hs,o}$ [℃]
Liao's law
T_3 [℃]
Optimal pressure
Liao
COP [-]
p_c [10^5 Pa]

Fig 9.

FIGURES CAPTIONS

Fig. 1. Flow circuit of the transcritical CO_2 cycle with IHX.

Fig. 2. p-h diagram of a transcritical CO_2 cycle with IHX heat exchanger.

Fig 3. Outlet gas cooler temperature as a function of the cycle high pressure and water inlet temperature for the baseline coaxial heat exchanger (heat exchanger “A” in Table 4). Optimal, Liao and Sarkar high pressure value curves are also plotted.

Fig 4. Cycle efficiency as a function of the cycle high pressure and water inlet temperature for the baseline coaxial heat exchanger (heat exchanger “A” in Table 3). Optimal, Liao and Sarkar high pressure value curves are also plotted.

Fig 5. Refrigerant gas cooler outlet temperature as a function of secondary fluid inlet temperature for different finned coil heat exchangers at different pressures together with Kauf and Chen and Gu correlations.

Fig. 6. Flow circuit of a commercial refrigeration transcritical CO_2 plant: (1) compressors, (2) gas cooler, (3) expansion valve, (4) liquid receiver, (5) refrigerated cabinets and cold rooms.

Fig. 7. Flow circuit of a CO_2 heat pump water heater: (1) compressor, (2) gas cooler, (3) expansion valve, (4) evaporator, (5) low pressure receiver, (6) internal heat exchanger.

Fig 8. Optimal and approximated correlations high cycle pressure as a function of secondary fluid inlet temperature for 25% and 100% compressor volumetric capacity for the commercial refrigeration plant.

Fig 9. Water and refrigerant gas cooler outlet temperature and COP as a function of high cycle pressure and water mass flow rate for the heat pump

water heater at 20℃ external air temperature and 15℃ gas cooler water inlet temperature.

TABLES

Table 1. Phenomenological coefficients used in numerical code.

	Heat Transfer	**Pressure Drop**	
		Localised	**Distributed**
	α [W/m^{2}K]	f [-]	ξ [-]
Air	Wang et al. [23]	Wang et al. [23]	Idelchik [24]
Water	Gnielinski [25]	Churchill [26]	Idelchik [24]
CO_2 Transcritical	Dang and Hihara [27]	Churchill [26]	Idelchik [24]
CO_2 Subcritical, two-phase evaporation	Cheng at al. [28]	Friedel [29]	Idelchik [24]
CO_2 Subcritical, single phase	Gnielinski [25]	Churchill [26]	Idelchik [24]

Table 2. Finned coil air cooled and coaxial water cooled gas coolers operating conditions and compressor characteristics.

		Finned coil	Coaxial
Evaporating pressure	[10^5 Pa]	26.5	34.9
Superheat	[K]	7.0	5.0
CO_2 mass flow rate	[kg/s]	0.500	0.067
Compressor isentropic efficiency	[-]	$1.003 - 0.121 \cdot (p_c/p_e)$	
Compressor volumetric efficiency	[-]	0.75	
Heat dissipation factor	[-]	0	

Table 3. Finned coil gas coolers geometric characteristics.

Finned coil gas cooler		**A**	**B**	**C**
Tube arrangement (material)			staggered (Cu)	
Longitudinal tube spacing (*)	[mm]		21.7	
Transverse tube spacing (**)	[mm]		25.0	
Inside tube diameter	[mm]		6.52	
Outside tube diameter	[mm]		8.52	
Inside tube surface			smooth	
Fins geometry (material)			plain (Al)	
Fin spacing	[mm]		2.1	
Fin thickness	[mm]		0.10	
Number of rows			4	
Number of tubes per row			88	
Number of circuits			44	
Tube length	[mm]	3200	1400	3200
Air mass flow rate	[kg/s]	14.69	6.43	6.43
Air face velocity	[m/s]	1.83	1.83	0.80

(*) Along the air flow (**) Normal to the air flow

Table 4. Coaxial gas coolers geometric characteristics.

Coaxial gas cooler		**A**	**B**	**C**
Refrigerant dislocation			shell	
Heat exchanger length	[m]		30	
Number of internal tubes	[-]		1	
Inner tube internal diameter	[mm]		12.0	
Inner tube external diameter	[mm]		14.0	
Outer tube internal diameter	[mm]		18.0	
Water mass flow rate	[kg/s]	0.090	0.074	0.113

Table 5. Finned coil gas coolers simulation results.

	Optimal (numerical solution)			**Liao**			**Sarkar**			**Kauf**			**Chen and Gu**		
$T_{hs,i}$	T_3	p_c	COP	T_3	Δp_c	ΔCOP	T_3	Δp_c	ΔCOP	T_3	Δp_c	ΔCOP	T_3	Δp_c	ΔCOP
[℃]	[℃]	[10^5 Pa]	[-]	[℃]	[10^5 Pa]	[%]	[℃]	[10^5 Pa]	[%]	[℃]	[10^5 Pa]	[%]	[℃]	[10^5 Pa]	[%]
A															
25	26.0	74.9	2.48	-	-	-	-	-	-	-	-	-	-	-	-
27	28.2	76.9	2.26	29.7	-1.9	-2.5	29.6	-1.8	-2.2	-	-	-	-	-	-
30	31.1	81.4	1.95	31.8	-1.6	-1.4	31.7	-1.3	-1.0	-	-	-	-	-	-
35	35.7	89.9	1.51	35.8	-1.1	-0.3	35.7	-0.2	0.0	35.6	1.1	-0.3	35.1	10.0	-8.3
40	40.4	98.9	1.16	40.4	0.1	0.0	40.3	1.9	-0.4	40.2	5.1	-2.3	40.1	12.6	-9.2
B															
25	33.5	86.4	1.70	33.9	-2.0	-0.3	33.8	-1.4	-0.1	-	-	-	-	-	-
27	34.8	89.9	1.57	35.2	-2.5	-0.3	35.1	-1.7	-0.1	-	-	-	34.9	-8.4	-5.6
30	37.1	93.9	1.39	37.3	-1.9	-0.1	37.2	-0.8	0.0	34.2	-15.9	-22.6	37.4	-5.5	-2.1
35	41.0	99.9	1.13	40.9	0.3	0.0	40.8	2.1	-0.2	40.5	-8.9	-6.4	41.0	0.0	0.0
40	44.9	106.9	0.91	44.9	2.1	-0.2	44.7	4.6	-1.0	44.9	-2.9	-0.5	44.7	4.5	-0.9
C															
25	28.6	81.9	2.09	31.1	-3.8	-3.0	30.9	-3.5	-2.7	-	-	-	-	-	-
27	30.7	83.9	1.92	32.3	-3.1	-2.4	32.1	-2.7	-2.0	-	-	-	-	-	-
30	33.1	88.4	1.69	34.2	-3.2	-1.7	34.1	-2.6	-1.1	-	-	-	-	-	-
35	37.3	95.9	1.35	37.8	-2.7	-0.7	37.6	-1.6	-0.2	38.1	-4.9	-2.8	36.6	4.1	-1.7
40	41.7	102.9	1.08	41.8	-0.7	0.0	41.6	1.0	0.0	41.6	1.1	-0.1	41.0	8.6	-4.3

Table 6. Coaxial gas coolers simulation results.

	Optimal (numerical solution)			**Liao**			**Sarkar**			**Kauf**			**Chen and Gu**		
$T_{hs,i}$	T_3	p_c	COP	T_3	Δp_c	ΔCOP	T_3	Δp_c	ΔCOP	T_3	Δp_c	ΔCOP	T_3	Δp_c	ΔCOP
[℃]	[℃]	[10^5 Pa]	[-]	[℃]	[10^5 Pa]	[%]	[℃]	[10^5 Pa]	[%]	[℃]	[10^5 Pa]	[%]	[℃]	[10^5 Pa]	[%]
								A							
10	21.2	77.5	4.07	-	-	-	-	-	-	-	-	-	-	-	-
15	23.2	83.4	3.53	30.1	-8.7	-5.4	30.1	-9.2	-5.4	-	-	-	-	-	-
20	26.1	89.1	3.04	32.2	-9.5	-4.3	32.2	-10.0	-4.3	-	-	-	-	-	-
25	30.0	94.1	2.62	34.5	-9.0	-4.7	34.5	-9.4	-4.7	-	-	-	-	-	-
30	34.0	99.1	2.24	37.1	-7.9	-4.2	37.1	-8.3	-4.0	-	-	-	37.2	-11.4	-6.9
35	37.9	104.8	1.89	39.9	-6.8	-2.9	39.9	-7.2	-2.7	39.8	-14.4	-11.0	39.5	-5.4	-1.6
								B							
10	27.2	79.9	3.44	30.1	-5.2	-2.3	30.1	-5.8	-2.3	-	-	-	-	-	-
15	29.4	85.3	3.00	32.0	-6.3	-2.1	29.4	-6.8	-2.2	-	-	-	-	-	-
20	32.3	90.0	2.62	34.1	-5.8	-2.3	32.3	-6.3	-2.3	-	-	-	-	-	-
25	34.6	96.4	2.27	36.4	-6.7	-2.4	34.5	-7.2	-2.3	-	-	-	-	-	-
30	37.2	102.7	1.97	39.0	-6.8	-2.6	37.2	-7.3	-2.5	-	-	-	38.4	-15.0	-8.2
35	39.8	111.0	1.69	41.7	-8.4	-1.5	39.9	-8.8	-1.3	40.7	-20.6	-11.2	41.9	-11.6	-2.6
								C							
10	12.2	76.1	4.79	-	-	-	-	-	-	-	-	-	-	-	-
15	17.6	79.9	4.12	-	-	-	-	-	-	-	-	-	-	-	-
20	22.7	84.1	3.52	-	-	-	30.5	-9.1	-6.3	-	-	-	-	-	-
25	27.6	88.7	2.97	-	-	-	32.9	-7.9	-6.0	-	-	-	-	-	-
30	32.4	93.4	2.50	32.5	-6.7	-5.0	35.4	-6.6	-4.9	-	-	-	35.1	-5.7	-3.4
35	36.5	99.8	2.07	36.5	-6.3	-3.2	38.3	-6.0	-2.9	38.7	-9.4	-7.7	36.6	-0.4	-0.1

Table 7. Commercial refrigeration plant and heat pump water heater operating conditions and compressor characteristics.

Commercial refrigeration plant		
Evaporation pressure	[10^5 Pa]	26.5
Superheat	[K]	7.0
Compressor volumetric capacity	[10^{-3} m^3/s]	10.0
Compressor isentropic efficiency	[-]	$0.795 - 0.037 \cdot (p_c/p_e)$
Compressor volumetric efficiency	[-]	$1.025 - 0.088 \cdot (p_c/p_e)$
Heat dissipation factor	[-]	0
Heat pump water heater		
Water outlet temperature	[℃]	60
Superheat	[K]	0.
Compressor volumetric capacity	[10^{-3} m^3/s]	0.972
Compressor isentropic efficiency	[-]	$0.762 - 0.047 \cdot (p_c/p_e)$
Compressor volumetric efficiency	[-]	$1.012 - 0.105 \cdot (p_c/p_e)$
Heat dissipation factor	[-]	0

Table 8. Commercial refrigeration plant simulation results.

	Optimal			**Liao**			**Sarkar**			**Kauf**			**Chen and Gu**		
$T_{hs,i}$	T_3	p_c	COP	T_3	Δp_c	ΔCOP	T_3	Δp_c	ΔCOP	T_3	Δp_c	ΔCOP	T_3	Δp_c	ΔCOP
[℃]	[℃]	[10^5 Pa]	[-]	[℃]	[10^5 Pa]	[%]	[℃]	[10^5 Pa]	[%]	[℃]	[10^5 Pa]	[%]	[℃]	[10^5 Pa]	[%]
Compressor volumetric capacity 100%															
25	26.0	75.4	2.57	-	-	-	-	-	-	-	-	-	-	-	-
27	27.9	77.9	2.38	-	-	-	-	-	-	-	-	-	-	-	-
30	30.7	82.9	2.12	31.5	-2.3	-1.3	31.7	-2.7	-2.1	-	-	-	-	-	-
35	35.4	91.9	1.72	35.4	-0.5	-0.1	35.6	-2.4	-0.7	35.5	-0.9	-0.2	35.1	8.0	-3.4
40	40.2	101.9	1.40	40.1	2.6	-0.2	40.2	-1.4	-0.1	40.1	2.1	-0.1	40.0	9.5	-2.5
Compressor volumetric capacity 75%															
25	25.2	74.9	2.65	-	-	-	-	-	-	-	-	-	-	-	-
27	27.4	75.4	2.46	-	-	-	-	-	-	-	-	-	-	-	-
30	30.4	79.9	2.18	30.8	-1.3	-0.8	31.0	-1.6	-1.2	-	-	-	-	-	-
35	35.1	89.9	1.74	35.1	0.7	-0.2	35.2	-1.4	-0.2	35.1	1.1	-0.3	35.0	10.0	-4.7
40	40.0	100.9	1.41	40.0	3.4	-0.4	40.0	-0.8	0.0	40.0	3.1	-0.3	40.0	10.5	-2.9
Compressor volumetric capacity 50%															
25	25.0	75.0	2.66	-	-	-	-	-	-	-	-	-	-	-	-
27	27.0	75.0	2.51	-	-	-	-	-	-	-	-	-	-	-	-
30	30.1	77.5	2.24	30.2	-0.5	0.0	30.3	-0.7	-0.1	-	-	-	-	-	-
35	35.0	88.0	1.76	35.0	2.4	-0.5	35.0	0.1	0.0	35.0	3.0	-0.7	35.0	12.0	-5.4
40	40.0	100.0	1.41	40.0	4.3	-0.6	40.0	0.1	0.0	40.0	4.0	-0.5	40.0	11.5	-3.1
Compressor volumetric capacity 25%															
25	25.0	75.0	2.66	-	-	-	-	-	-	-	-	-	-	-	-
27	27.0	75.0	2.51	-	-	-	-	-	-	-	-	-	-	-	-
30	30.0	75.0	2.27	30.0	1.4	0.0	30.0	1.1	0.0	-	-	-	-	-	-
35	35.0	88.0	1.76	35.0	2.3	-0.5	35.0	0.0	0.0	35.0	3.0	-0.8	35.0	11.9	-5.6
40	40.0	100.0	1.41	40.0	4.3	-0.6	40.0	0.1	0.0	40.0	4.0	-0.5	40.1	11.5	-3.4

Table 9. Heat pump evaporator and IHX characteristics.

Finned coil evaporator		
Tube arrangement (material)		In-line (Cu)
Outside tube diameter	[mm]	9.52
Number of rows	[-]	4
Air side heat transfer area	[m^2]	82.3
Tube side heat transfer area	[m^2]	6.8
Face area	[m^2]	1.7
Air face velocity	[m/s]	1.04
Coaxial IHX		
Low pressure dislocation		shell
Tube side heat transfer area	[m^2]	0.26
Shell side heat transfer area	[m^2]	0.38
Tube side flow area	[m^2]	$3.85\ 10^{-4}$
Shell side flow area	[m^2]	$1.34\ 10^{-3}$

Table 10. Heat pump water heater simulation results.

	Optimal					**Liao**					**Sarkar**				
$T_{hrs,i}$ [℃]	p_c [10^5 Pa]	T_3 [℃]	T_e [℃]	$\dot{m}_{hs}$ [kg/s]	COP [-]	Δp_c [10^5 Pa]	T_3 [℃]	T_e [℃]	$\dot{m}_{hs}$ [kg/s]	ΔCOP [%]	Δp_c [10^5 Pa]	T_3 [℃]	T_e [℃]	$\dot{m}_{hs}$ [kg/s]	ΔCOP [%]
$T_{hs,i}$ = 15 ℃															
-10	82.1	16.2	-15.4	0.06	2.04	-	-	-	-	-	-	-	-	-	-
0	86.2	18.1	-6.3	0.08	2.69	-7.7	31.5	-5.1	0.06	-15.3	-7.6	31.5	-5.1	0.06	-14.9
10	91.4	17.6	2.6	0.10	3.50	-11.7	32.5	4.5	0.07	-18.2	-11.7	32.7	4.5	0.07	-18.2
20	97.9	17.7	11.81	0.13	4.59	-13.9	34.3	13.5	0.10	-14.6	-	-	-	-	-
$T_{hs,i}$ = 30 ℃															
-10	90.0	30.4	-14.5	0.08	1.54	-	-	-	-	-	-	-	-	-	-
0	91.3	30.6	-5.5	0.10	2.07	-12.3	31.8	-5.4	0.08	-21.2	-12.2	31.7	-5.4	0.08	-21.3
10	93.0	31.7	3.6	0.13	2.74	-9.0	34.5	5.6	0.09	-30.1	-9.0	34.8	5.6	0.09	-30.1
20	97.8	31.5	12.9	0.16	3.67	-7.2	37.6	13.8	0.13	-10.3	-	-	-	-	-